Available online at www.sciencedirect.com
SCIENCE DIRECT®
Journal of Molecular Graphics and Modelling 23 (2005) 373–380
Journal of Molecular Graphics and Modelling
www.elsevier.com/locate/JMGM

Construction of a 3D model of nattokinase, a novel fibrinolytic enzyme from *Bacillus natto* A novel nucleophilic catalytic mechanism for nattokinase

Zhong-liang Zheng[a], Zhen-yu Zuo[a], Zhi-gang Liu[a], Keng-chang Tsai[b], Ai-fu Liu[a,1], Guo-lin Zou[a,*]

[a]*Key Laboratory of Virology (Wuhan University), Ministry of Education, Life Science's College of Wuhan University, Wuhan 430072, China*
[b]*Department of Life Science, National Tsing Hua University, Hsinchu 30043, Taiwan*

Received 7 July 2004; received in revised form 28 September 2004; accepted 11 October 2004
Available online 15 December 2004

Abstract

A three-dimensional structural model of nattokinase (NK) from *Bacillus natto* was constructed by homology modeling. High-resolution X-ray structures of Subtilisin BPN' (SB), Subtilisin Carlsberg (SC), Subtilisin E (SE) and Subtilisin Savinase (SS), four proteins with sequential, structural and functional homology were used as templates. Initial models of NK were built by MODELLER and analyzed by the PROCHECK programs. The best quality model was chosen for further refinement by constrained molecular dynamics simulations. The overall quality of the refined model was evaluated. The refined model NKC1 was analyzed by different protein analysis programs including PROCHECK for the evaluation of Ramachandran plot quality, PROSA for testing interaction energies and WHATIF for the calculation of packing quality. This structure was found to be satisfactory and also stable at room temperature as demonstrated by a 300 ps long unconstrained molecular dynamics (MD) simulation. Further docking analysis promoted the coming of a new nucleophilic catalytic mechanism for NK, which is induced by attacking of hydroxyl rich in catalytic environment and locating of S221.

Keywords: Nattokinase; Fibrinolytic enzyme; Homology modeling; Nucleophilic attack; Mechanism

1. Introduction

Nattokinase (NK) is a potent fibrinolytic enzyme from *Bacillus natto*. Closely resembling plasmin, NK dissolves fibrin directly. In addition, it also enhances the body's production of both plasmin and other clot-dissolving agents, including urokinase. In some ways, NK is actually superior to conventional clot-dissolving drugs, which has many benefits including convenience of oral administration, confirmed efficacy, prolonged effects, cost effectiveness and can be used preventatively. NK has demonstrated stability of pH and temperature so that it can occur stably in the gastrointestinal tract [1].

NK is a single-chain structure comprised of 275 amino acids and has no intramolecular disulfide bond [2]. Belonging to subtilisin family of serine protease, NK has the same conservative catalytic triad (D32, H64, S221) and oxyanion hole (N155) [3]. The binding sites (S125, L126, G127) of substrate also position the binding pockets S1 and S4 of subtilisin [4]. NK keeps highly homologous character with most of subtilisins and the 3D structures of many subtilisins have been obtained by using X-ray crystal diffraction and NMR. But the 3D structure of NK is still unknown.

The homology model for NK was generated by using the 3D structures of SB, SC, SE and SS, which was based on the sequence homology of 84.9%, 67.8%, 98.9% and 62.92% between NK and them. In order to understand the catalyzing mechanism and substrate specificity of NK, several substrates have been docked into the active site of the model

* Corresponding author. Tel.: +86 27 87645674.
E-mail address: zouguolin@whu.edu.cn (G.-l. Zou).
[1] Co-corresponding author.

1093-3263/$ – see front matter © 2004 Elsevier Inc. All rights reserved.
doi:10.1016/j.jmgm.2004.10.002

structure with Lamarckian Genetic Algorithm. The interaction between NK and substrates has been determined by calculating the hydrogen bonds of the binding site for the enzyme–substrate complexes. Based on our work, we attempt to explain the interrelation between the structure and the function of NK.

2. Methodology

2.1. Sequence and structure alignment

Sequence of NK was from NCBI protein database (GenBank accession no. is S51909). Sequences and structures of SB, SC, SE and SS, all from *Bacillus subtilus* family, were obtained from the RSCB protein data bank (PDB ID are 1AU9, 1AF4, 1SCJ and 1GCI, respectively). Sequence alignment was derived using the CLUSTAL W program, and default parameters were applied [5]. Structure alignment was obtained and analyzed by using GRASP package with default parameters [6]; and both aligned results were inspected and adjusted manually to minimize the number of gaps and insertions.

2.2. Rough model

Sequence alignment between NK and SB, SC, SE and SS was used to drive a 3D model for NK. Five rough 3D models based on multiple templates were constructed by using the academic version 6.2 of MODELLER [7,8] with the default parameters that proposed loop conformations. The qualities of the models were analyzed by PROCHECK3.5 [9]. Secondary structures were assigned and compared by GRASP package. Secondary structure of NK was also predicted by the Ph.D. [10] program. PROCHECK results and the extent of secondary structural elements in comparison with the Ph.D. prediction were carefully analyzed for the models. The best model (Model C) was chosen and the quality of structure was displayed in Table 1. Model C had the better Ramachandran plot and the more extent secondary structural motifs so that it was chosen for the further refinement.

2.3. Refinement and MD simulation

Model C was first refined by adding all hydrogen atoms and underwent energy minimization with the SANDER module of AMBER 7 [11], using the PARM99 force field. WATERBOX216 unit was added to form an octahedron system and 8 Å cut-off was adopted for non-bonded interactions. The minimization protocol included 2500 steps of steepest descent, followed by 2500 steps of conjugate gradients. A harmonic constraint of 100 kJ/mol/Å^2 was applied on all protein atoms [12]. A final refined model C1 was obtained after minimization. The quality of this model was examined by PROCHECK. We found that Model C1 has a better overall quality and better conserved secondary structures. So, Model C1 was chosen for further evaluation.

An MD simulation process was further applied for testing the stability of Model C1 at room temperature and at normal pressure. Model C1 was subjected to an unconstrained MD simulations at 300 K for 300 ps with a time step of 2.0 fs. The non-bonded cut-off was set to 8.0 Å.

2.4. Evaluation of refined model

The qualities of the final refined model from above steps were subjected to a series of tests for their internal consistency and reliability. Backbone conformation was evaluated by PROCHECK. The energy of residues was checked by PROSA2003 [13]. Finally, packing quality of the refined structure was investigated by the calculation of WHATIF [14] Quality Control value.

2.5. Docking

The ligands were H-D-VLK-pNA (SUB1) and Suc-AAPF-pNA (SUB2) [1,3], respectively. SUB1 is a chromogenic substrate for plasmin and streptokinase-activated

Table 1
Quality of structures checked by PROCHECK

Structure	Ramachandran plot quality (%)				Goodness factor		
	Core	Allowed	General	Disallowed	Dihedrals	Covalent	Overall
SB	87.8	11.3	0.5	0.5	−0.05	−2.51	−1.05
SC	86.7	12.4	0.9	0.0	0.09	0.33	0.20
SE	88.5	11.0	0.4	0.0	−0.11	0.16	0.01
SS	88.5	11.0	0.4	0.0	−0.11	0.16	0.01
NKA	87.2	11.5	1.3	0.0	−0.25	0.16	−0.07
NKB	89.9	9.7	0.4	0.0	0.09	−0.08	0.02
NKC	89.9	10.1	0.0	0.0	0.07	−0.11	0.00
NKD	89.4	10.1	0.4	0.0	0.09	−0.10	0.02
NKE	88.1	11.9	0.0	0.0	0.11	−0.10	0.03
NKC1	91.2	8.8	0.0	0.0	0.09	−0.13	0.00

Ramachandran plot qualities show the amount (%) of residues belonging to the core, allowed, generally allowed and disallowed region of the plot; goodness factors show the quality of covalent and overall bond/angle distances; these scores should be above −0.5 for a reliable model.

plasminogen and is the optimum substrate for NK. The docking was performed in two steps. First, the ligands were arbitrarily positioned in the active center of Model C1 by using DEEP-VIEW [15]. The model was previously protonated with polar hydrogen and the partial charges added by AutoDockTools (ADT, the graphical front-end of AutoDock and AutoGrid) [16] as well as the solvation parameters. Then the plausible dockings were found with the widely used program AUTODOCK3.05 [17–19]. Automated docking simulations start with a ligand molecule in an arbitrary conformation orientation, and positions and finds favorable dockings in a protein-binding site, using Lamarckian Genetic Algorithm [19]. Interaction energies are calculated with a free-energy-based expression. The force field was calibrated with chemically diverse protein/ligand complexes of a known structure. Finally, the lowest energy conformers obtained were analyzed comparing the orientation of the substrate relative with the catalytic triad (D32, H64, S221).

3. Results and discussion

3.1. Homology modeling

The final alignment of NK sequence to those of SB, SC, SE and SS is shown in Fig. 1. As many Bacillus subtilisins, NK has the identity of sequence length including 275 amino acids. So, the consequence of gap would not be considered. Conserved domain of NK was detected in NCBI and is the same as the common secondary structures determined by GRASP package. It is interesting that Ph.D. also predicts the same key structures including the catalytic triad (D32, H64, S221). The sequence identity of the catalytic domain is as high as 99%, which suggests the most important part of the sequence for catalytic activity is most conserved. The binding pocket also has the sequence identity above 90%. Therefore, we conclude that this alignment can be used to construct a reliable 3D model for NK.

The results of PROCHECK analysis for the models are collected in Table 1. Comparing with four templates, Models A–E have the similar quality of Ramachandran plots, which are acceptable for the relatively low percentage of residues having disallowed torsional angels. Secondary structures of Models A–E have been investigated by GRASP package, and we found that Model C has more extent secondary structures and better stereochemistry character, which allows further refinement.

Model C1 minimized from Model C was finally selected as the best refined one. First, the quality of residue backbone conformations in Model C1 was checked by PROCHECK. As shown in Table 1, the quality of the Ramachandran plot as well as the goodness factors was found to be better than those of Model C. The distribution of the Ψ/Φ angles of Model C1 is all within the allowed regions. And no residues have disallowed conformations (Fig. 2). Thus, the above analysis suggests the backbone conformations of Model C to be better than those of the templates. Second, the interaction energy of each residue was checked by using PROSA. From Fig. 3, we can see that the residue energies of Model C1, including pair energy, combined energy and surface energy, are all negative. And compared with templates, Model C1 has the similar energy tendency as shown in Fig. 4. So, we can see that Model C1 reaches the energy criteria of PROSA. Third, the packing quality of each residues of Model C1 also reaches the criteria of WHATIF, because there is no score lower than −5.0 in the structure of Model C1 as shown in Fig. 5. The overall stability of the model structure was finally

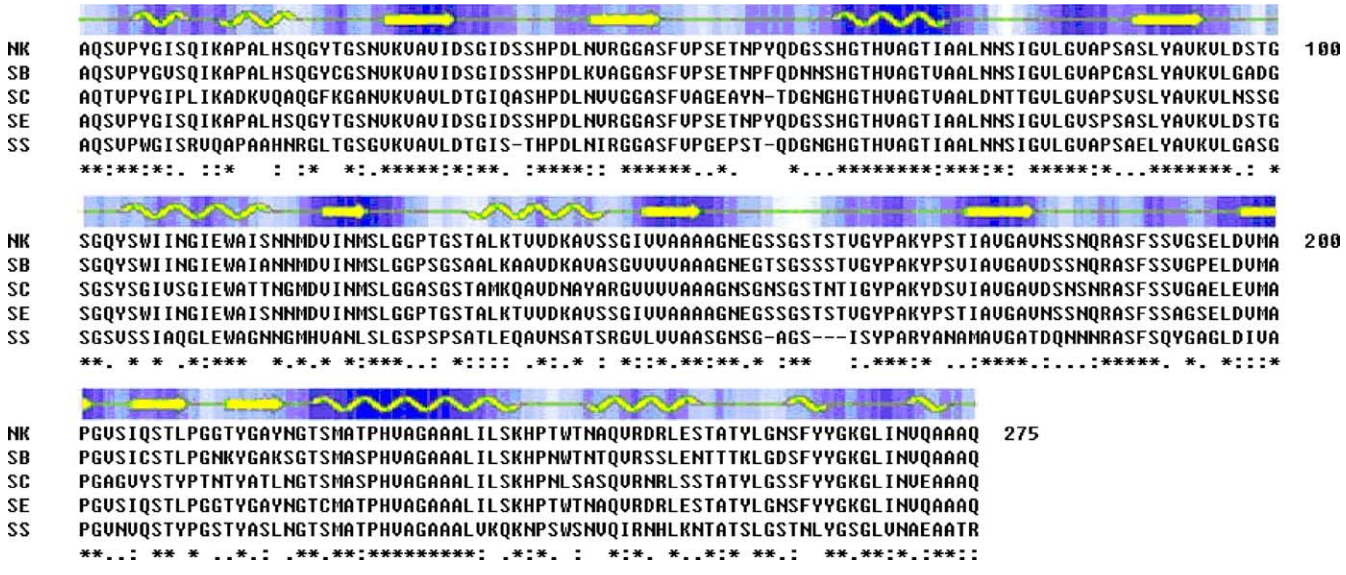

Fig. 1. The sequence alignment of NK, SB, SC, SE and SS produced by CLUSTAL W. The common secondary structure of SB, SC, SE and SS was produced by GRASP and is shown with arrows for β-sheet and spirals for α-helix. The background of the structure alignment reflects the solvent accessibility of the amino in the common secondary structure on a scale of black for buried to white for solvent accessible.

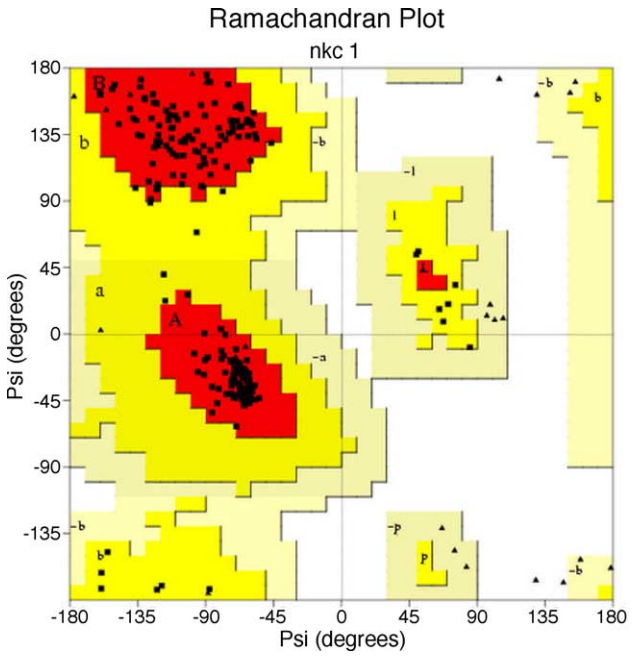

Fig. 2. Ramachandran plot of the Ψ/Φ distribution of Model C1 produced by PROCHECK: 91.2% residues are in most favored regions; 8.2% residues are in additional allowed regions.

investigated by using an unconstrained MD simulation. Result shows that total, potential and kinetic energies are always remained constant during the simulation and the protein size also remained constant. It can be seen that the system remains in equilibrium during the entire simulation. Then, we concluded that Model C1 is stable at room temperature.

In summary, the quality of the backbone conformation, the residue interaction, the residue contact and the dynamic stability of the structure are all well within the limits established for reliable structures. Passing all tests by Model C1 suggests that an adequate model for NK is obtained to

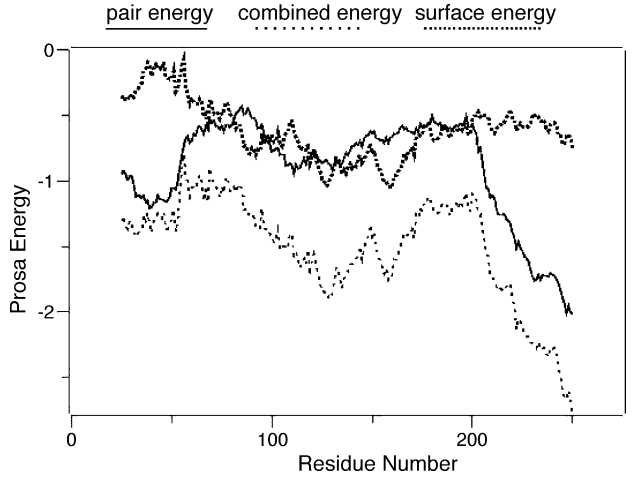

Fig. 3. Prosa energy profiles calculated for Model C1. The values of pair energy, surface energy and combined energy should be under 0 for a reliable model.

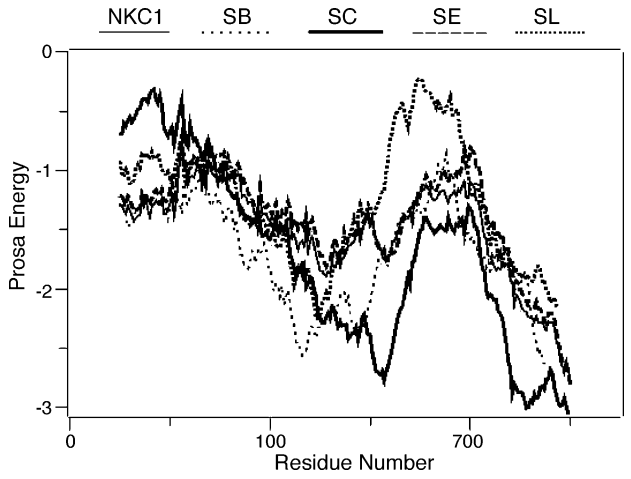

Fig. 4. Prosa energy profiles calculated for Model C1, SB, SC, SE and SL. The value of energy should be under 0 for a reliable model.

characterize protein–substrate interactions and to investigate the relation between the structure and function.

3.2. Docking of substrates to NK

Similar to other subtilisins, the catalytic center of NK, including the catalytic triad (D32, H64, S221) [20] and oxyanion hole (N155) [21] is positioned in the pocket constructed by two α-helix and seven β-strand. As shown in Figs. 6 and 7, two substrates were docked into the active center of Model C1 by using the program AUTODOCK3.05. We chose the widely docking parameters [22], which were 150 for ga_pop_size, 10,000,000 for ga_num_evals. Amazingly, after 100 calculating cycles, we found out that both of the peptide bonds formed by the amido of *p*-nitroaniline are located in the center of oxyanion hole. And the whole peptide bond of two substrates are exposed directly to the interaction of H64, S221 and N155, which further verify the accuracy of the conformation of the catalytic center. Here we

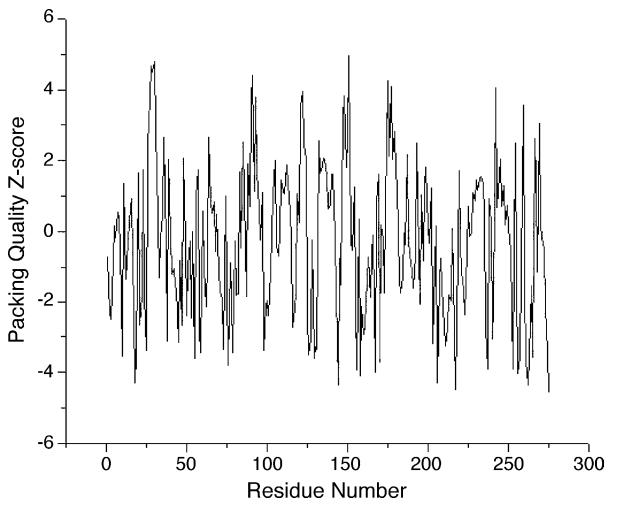

Fig. 5. WHATIF quality control values calculated for Model C1. The scores should be above −5 for a reliable model.

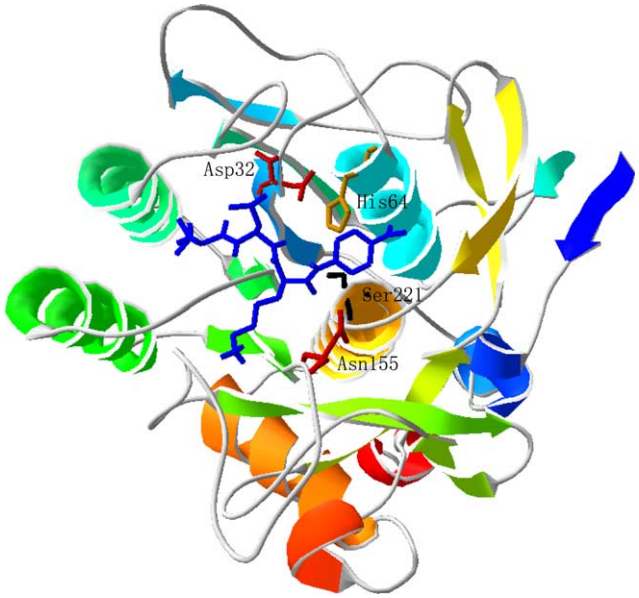

Fig. 6. SUB1 docked to active center of NK (Model C1) using Autodock3.05. SUB1 is colored blue and shown with the stick rendering. The catalytic triad (D32, H64, S221) and oxyanion hole (N155) are colored by custom scale, labeled by their residue name, and shown with the stick rendering. The backbone of NK (Model C1) is colored by secondary structures. Some residues were moved for clarity. This figure was made by DeepView v3.7.

name these two peptide bonds formed by the amido of *p*-nitroaniline as active peptide bond (APB).

Analyzing the electrostatic potentials of active centers of NK, SB, SC, SE and SS, we found that the overall active center of NK is more negative than others and negative electrostatic region mainly concentrates around the binding pocket S1 and S4. This suggests that NK possesses a higher specificity for the substrates showing positive charges. We added all-H and Gasteiger charges to two substrates by using ADT, and got the net charge 0.9995 for SUB1 and −2.0005 for SUB2. As shown in Figs. 8 and 9, SUB1 is docked into the binding pocket S1 and S4 of NK, while SUB2 is not. So we concluded that as the optimum substrate for NK, SUB1 shows the more stable and actual docking state in Fig. 6; and within the binding pocket S1 and S4 of NK, the electrostatic potential is mainly caused by E156, which carries negative charges. So the residue of E156 will act on the residue carrying positive charges in substrates. As shown in Fig. 8, the residue of lysine from SUB1 carrying positive charges can form two hydrogen bonds with the residue of E156. Other residues of the binding pocket S1 and S4 of NK are mostly hydrophobic amino acids, which suggests that these residues will act on hydrophobic residues of substrates. From Fig. 8, we can see that residues G102 and G127 are very close to the leucine of SUB1 and residues Y104 and I107 are also very close to the valine of SUB1. We think it must be hydrophobic interaction that makes the leucine and the valine of SUB1 bind with residues G102, Y104, I107 and G127. Then, we concluded that the main binding sites of NK for SUB1 may be G102, Y104, I107, G127 and E156.

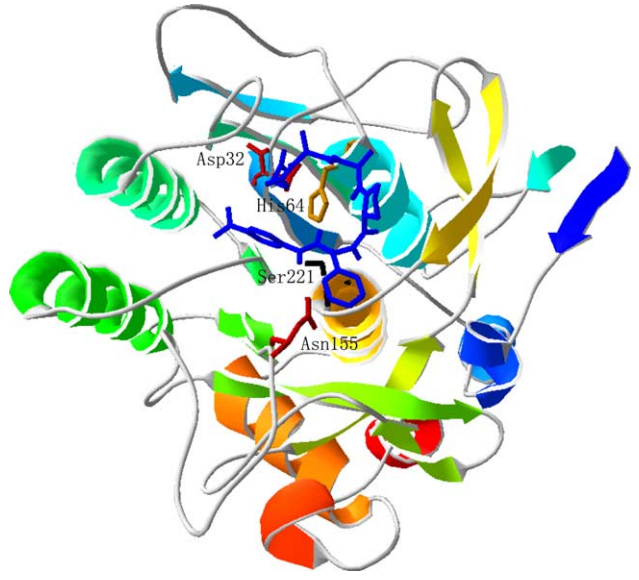

Fig. 7. SUB2 docked to active center of NK (Model C1) using Autodock3.05. SUB2 is colored blue and shown with the stick rendering. The catalytic triad (D32, H64, S221) and oxyanion hole (N155) are colored by custom scale, labeled by their residue name, and shown with the stick rendering. The backbone of NK (Model C1) is colored by secondary structures. Some residues were moved for clarity. This figure was made by DeepView v3.7.

Further analysis of hydrogen-bond interactions shows that the carboxyl of D32 has the trend to form two hydrogen bonds with the sp^3 nitrogen of H64. When considering the rotation of the residue of S221, we found the hydroxyl of S221 can also form hydrogen bonds with the sp^2 nitrogen of H64 [23]. We checked the same catalytic triad of other subtilisins, and the same property was found. This suggests that hydrogen bonds among the catalytic triad play an important role in hydrolyzation of peptide bonds [24].

The interactions between substrates and residues of the active center of NK were also analyzed carefully. To our surprise, we found that the hydroxyl of S221 has a trend to form a hydrogen bond with the nitrogen of SUB1's APB as shown in Fig. 8, and the distance is 2.84 Å. The sp^2 nitrogen of H64 has a trend to form a hydrogen bond with the oxygen of SUB2's APB as show in Fig. 9, and the distance is 2.85 Å. But the forming of the two foregoing hydrogen bonds deviates from the catalytic mechanism put forward by Carter and Wells [20] as show in Fig. 10. Carter and Wells think that H64 accepts a proton from S221 and subsequently donates it to the leaving group amine to promote acylation in the mechanism of wild-type subtilisin. In deacylation, H64 is thought to act as a general base by removing a proton from water leading to nucleophilic attack upon the acyl-enzyme and finally to reprotonation of S221.

NK had evolved a similar catalytic device as other subtilisins. So, the catalytic triad and the oxyanion hole of NK should have the same catalytic behavior. But NK has different characters in physics and chemistry. So we

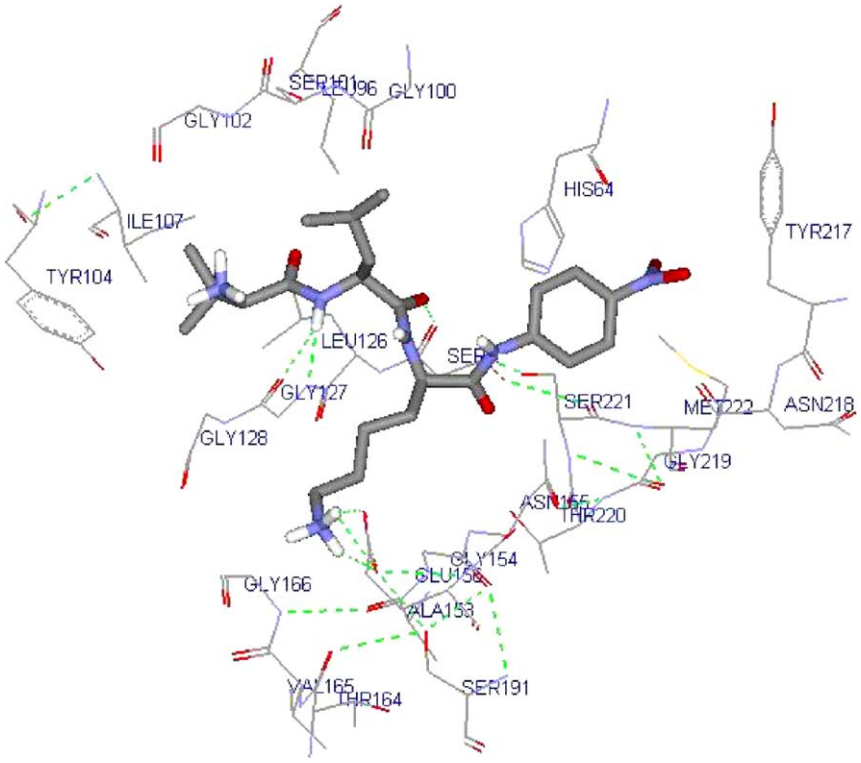

Fig. 8. The hydrogen-bond interaction between SUB1 and the catalytic triad (D32, H64, S221) of NK (Model C1). SUB1 is colored by atom and shown with the stick rendering. The residues from NK (Model C1) are colored by atom, labeled by their residue name and shown with the line rendering.

supposed, if the two-foreging hydrogen bonds actually exist, NK possibly has an independent catalytic mechanism.

After studying the kinetics data [20,26] of Carter and Wells, we have some different points for the catalytic mechanism of NK. First, we think that hydroxyl rich in alkaline environment can also act as nucleophile to attack APB. Thomas et al. [25] proved that the ability of H64 for accepting a proton from S221 lies on alkaline pH and catalytic activity varies with pH following the ionization of this residue. But, in the kinetics data [20,26], we found that k_{cat} of the enzyme lacking H64 or D32 at pH 9.70 is 5.1- or 7.8-fold higher than that at pH 8.6 and these values are 3.6- to 5.6-fold higher than that of wild type enzyme. We know that the proton from S221 cannot be transformed without the assistance of D32 and H64. But why is the increasing fold of k_{cat} of enzyme lacking D32 or H64 higher than that of wild type enzyme? The principle of Carter and Wells cannot explain it. We suppose it is the action of hydroxyl rich in alkaline environment, because the ability of H64 for accepting a proton is determined by the ability of D32 for providing electrostatic interaction by forming the conjugated π bond from the dissociative carboxyl of D32. But the ability of D32 for forming the conjugated π bond will not always increase with the increasing of pH of environment because the dissociative carboxyl of D32 has only one proton for being snatched by hydroxyl in solution.

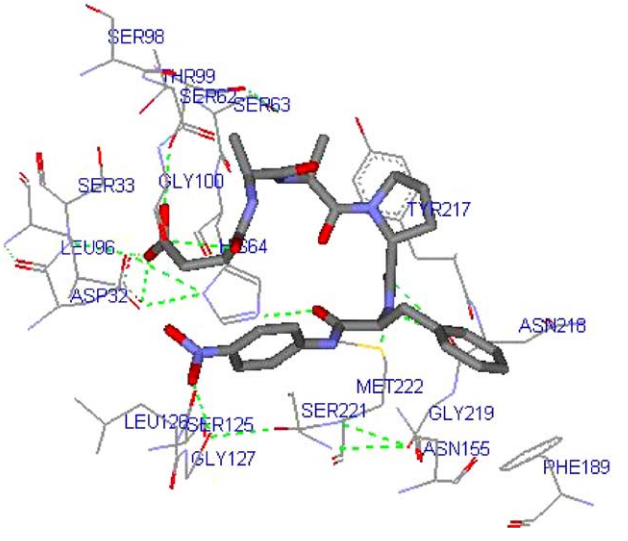

Fig. 9. The hydrogen-bond interaction between SUB2 and the catalytic triad (D32, H64, S221) of NK (Model C1). SUB2 is colored by atom and shown with the stick rendering. The residues from NK (Model C1) are colored by atom, labeled by their residue name and shown with the line rendering.

Second, how does APB locate stably in the center of oxyanion hole? And how does the hydroxyl of S221 recognize the carbon atom of APB. The principle of Carter and Wells cannot also explain these questions. However, after further analyzing the kinetics data [25] of Carter and Wells, we found that k_{cat} of the enzyme lacking S221 is 10- to 400-fold lower than that of the enzyme lacking D32 or

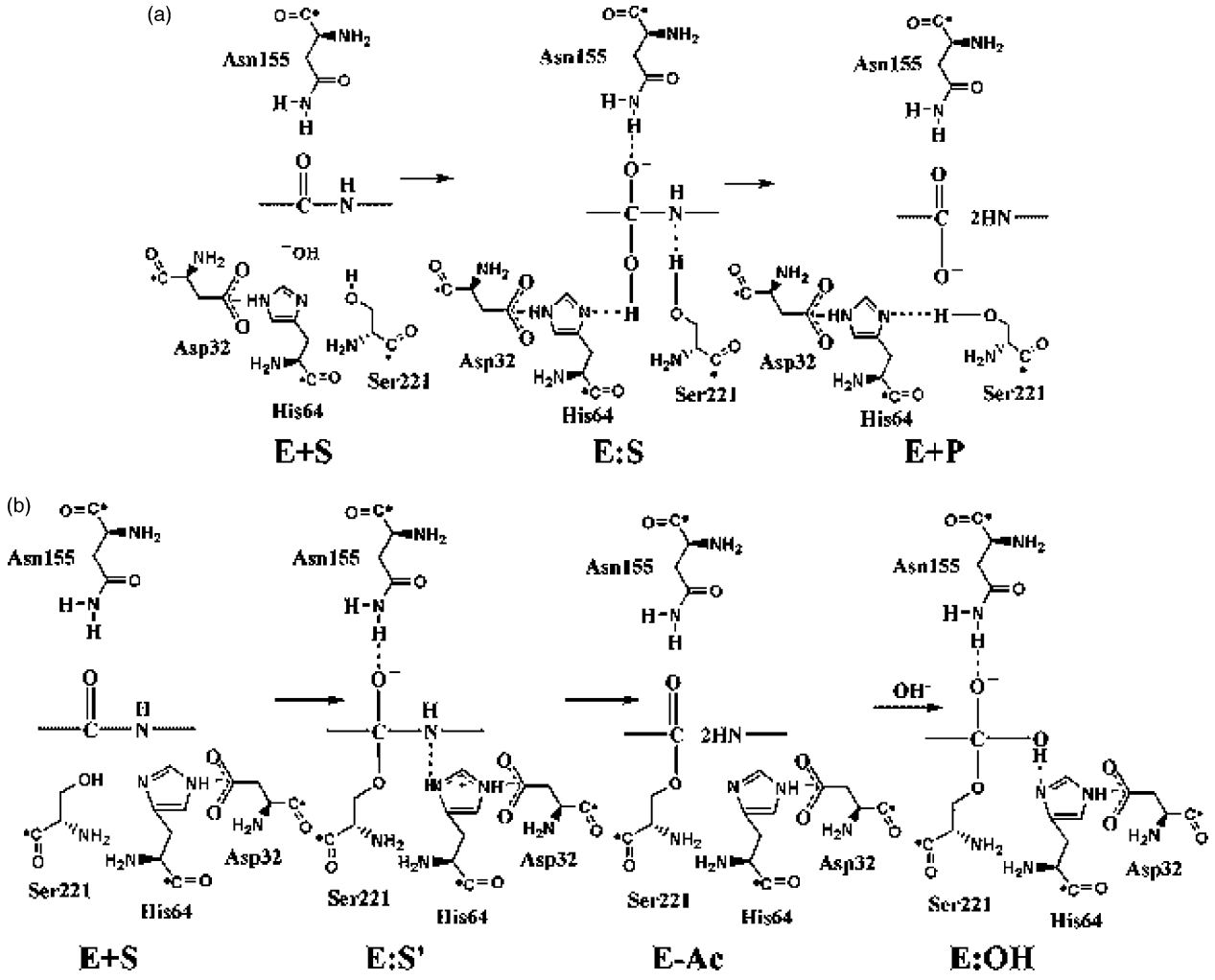

Fig. 10. Schematic diagram showing the nucleophilic attack steps put forward by us (diagram a) and by Carter and Wells (diagram b). Diagram a shows that the nucleophilic attack is introduced by hydroxyl rich in catalytic environment and only one transition state complex (E:S) is formed. Diagram b shows that the nucleophilic attack is introduced by the hydroxyl of S221. There are two transition state complexes formed. One is E:S, another is E:OH.

H64. K_m of the enzyme lacking S221 is 2- to 4-fold higher than that of the enzyme lacking D32 or H64. And k_{cat}/K_m of the enzyme lacking S221 is 10- to 200-fold lower than that of the enzyme lacking D32 or H64. We know that $1/K_m$ means the affinity to substrates and k_{cat}/K_m means the specificity of enzyme. The kinetics data of Carter and Wells proves that S221 plays an important role not only in catalysis but also in location of APB [27].

Third, does the sp^2 nitrogen of H64 activated by the conjugated π bond of D32 really have enough basicity to break the oxygen–hydrogen bond from S221? We do not think so. pK_a of the oxygen–hydrogen bond from S221 is 15.9 almost the same as that of water, which suggests that leaving of proton from S221 must stride an upper bond energy. Moreover, if the proton from S221's hydroxyl can be snatched easily by H64, the oxygen from S221's hydroxyl will be easily oxidized by oxidant in catalytic environment. Thus, the active center of subtilisin will be very unstable.

Based on the above discussion, we put forward a new nucleophilic catalytic mechanism for NK, and the critical nucleophile is hydroxide ions rich in environment. As shown in Fig. 10, in alkaline environment, APB is stably located in the center of oxyanion hole by two hydrogen bonds. One is between the hydroxyl of S221 and the nitrogen atom of APB; the other is between the acyl-amidocyanogen of N155 and the oxygen atom of APB. Then nucleophilic attacks to the carbon atom of APB by hydroxyl rich in environment are taking place with the help of H64. System goes into an unstable transitional state. With the break of APB, the proton of S221 is transferred to the nitrogen atom of APB. At the same time, H64 snatches the proton of the hydroxyl and transfers it to S221. Finally, the charges of the system reach to balance and hydrolyzation terminates.

In our principle for catalytic mechanism of NK, we emphasize more on the action of hydroxyl rich in catalytic environment and the action of S221 for locating APB. The detailed structure and function of the active center of NK is being determined by energetics and kinetics. Further experiment will supply enough proof for the validity of our principle.

Acknowledgements

This work is mainly supported by the National Natural Scientific Foundation (39770200) and supported in part by a grant from the National Science Council, Taiwan (NSC92-2313-B-007-002). The AMBER studies are conducted at the National Center for High Performance Computing, Taiwan. We are grateful to Dr. Keng-chang Tsai for his fruitful discussions concerning the structural interpretation of enzyme–substrate complexes.

Appendix A. Supplementary data

Supplementary data associated with this article can be found, in the online version, at doi:10.1016/j.jmgm.2004.10.002.

References

[1] H. Sumi, A novel fibrinolytic enzyme in the vegetable cheese natto: a typical and popular soybean food in the Japanese diet, Experientia 43 (20) (1987) 1110–1111.
[2] T. Nakamura, Y. Yamagata, E. Ichishima, Nucleotide sequence of the subtilisn NAT gene, aprN of Bacillus Subtilis (natto), Biosci. Biotech. Biochem. 56 (11) (1992) 1869.
[3] P. Yong, H. Qing, Z. Ren-huai, Z. Yi-zheng, Purification and characterization of a fibrinolytic enzyme produced by *Bacillus amyloliquefaciens* DC-4 screened from *douchi*, a traditional Chinese soybean food, Comp. Biochem. Physiol. 134 (2003) 45–52.
[4] P.N. Bryan, Protein engineering of subtilisin, Biochim. Biophys. Acta 1543 (2000) 203–222.
[5] D. Higgins, J. Thompson, T. Gibson, J.D. Thompson, D.G. Higgins, T.J. Gibson, CLUSTAL W: improving the sensitivity of progressive multiple sequence alignment through sequence weighting, position-specific gap penalties and weight matrix choice, Nucleic Acids Res. 22 (1994) 4673–4680.
[6] A. Nicholls, K. Sharp, B. Honig, Graphical representation and analysis of structural properties, Proteins Struct. Funct. Genet. 11 (4) (1991) 281.
[7] A. Sali, T.L. Blundell, Comparative protein modeling by satisfaction of spatial restraints, J. Mol. Biol. 134 (1993) 779–815.
[8] R. Sanchez, A. Sali, Advances in comparative protein-structure modeling, Curr. Opin. Struct. Biol. 7 (1997) 206–214.
[9] R.A. Laskowski, M.W. MacArthur, D.S. Moss, J.M. Thornton, PROCHECK: a program to check the stereo chemical quality of protein structures, J. Appl. Cryst. 26 (1993) 283–291.
[10] B. Rost, C. Sander, Prediction of protein secondary structure at better than 70% accuracy, J. Mol. Biol. 232 (1993) 584–599.
[11] D.A. Case, D.A. Pearlman, J.W. Caldwell, T.E. Cheatham, J.M. Wang, W.S. Ross, C. Simmerling, T. Darden, K.M. Merz, R.V. Stanton, A. Cheng, J.J. Vincent, M. Crowley, V. Tsui, H. Gohlke, R. Radmer, Y. Duan, J. Pitera, I. Massova, G.L. Seibel, U.C. Singh, P. Weiner, P.A. Kollman, AMBER 7, University of California, San Francisco, 2002.
[12] J. Wang, P. Cieplak, P.A. Kollman, How well does a restrained electrostatic potential (RESP) model perform in calculating conformational energies of organic and biological molecules? J. Comput. Chem. 21 (12) (2000) 1049–1074.
[13] M.J. Sippl, Boltzmann's principle, knowledge based mean fields and protein folding, an approach to the computational determination of protein structures, J. Comput. Aided Mol. Des. 7 (1993) 473–501.
[14] R.W.W. Hooft, G. Vriend, C. Sander, E.E. Abola, Errors in protein structures, Nature 381 (1996) 272.
[15] N. Guex, M.C. Peitsch, SWISS-MODEL and the Swiss-Pdb Viewer: an environment for comparative protein modeling, Electrophoresis 18 (1997) 2714–2723.
[16] M.F. Sanner, B.S. Duncan, C.J. Carrillo, A.J. Olson, Integrating computation and visualization for biomolecular analysis: an example using Python and AVS, Proc. Pac. Symp. Biocomput. 99 (1998) 401–412.
[17] D.S. Goodsell, A.J. Olson, Automated Docking of Substrates to Proteins by Simulated Annealing, Proteins Struct. Funct. Genet. 8 (1990) 195–202.
[18] G.M. Morris, D.S. Goodsell, R. Huey, A.J. Olson, Distributed automated docking of flexible ligands to proteins: parallel applications of Autodock 2.4, J. Comput. Aided Mol. Des. 10 (1996) 293–304.
[19] G.M. Morris, D.S. Goodsell, R.S. Halliday, R. Huey, W.E. Hart, R.K. Belew, A.J. Olson, Automated docking using Lamarckian genetic algorithm and an empirical binding free energy function, J. Comp. Chem. 19 (1998) 1639–1662.
[20] P. Carter, J.A. Wells, Dissecting the catalytic triad of a serine protease, Nature 332 (7) (1988) 564–568.
[21] P. Bryan, M.W. Pantoliano, S.G. Quill, H.Y. Hsiao, T. Poulos, Site-directed mutagenesis and the role of the oxyanion hole in subtilisin, Proc. Natl. Acad. Sci. U.S.A. 83 (1986) 3743–3745.
[22] O.V. Buzko, A.C. Bishop†, K.M. Shokat, Modified AutoDock for accurate docking of protein kinase inhibitors, J. Comput. Aided Mol. Des. 16 (2002) 113–127.
[23] P. Kuhn, et al. The 0.78 Å structure of a serine protease: *Bacillus lentus* subtilisin, Biochemistry 37 (1998) 13446–13452.
[24] J.A. Wells, B.C. Cunningham, T.P. Graycar, D.A. Estell, Importance of hydrogen-bond formation in stabilizing the transition state of subtilisin, Philos. Trans. R. Soc. London 317 (1986) 415–423.
[25] P.G. Thomas, A.J. Russell, A.R. Fersht, Tailoring the pH dependence of enzyme catalysis using protein engineering, Nature 318 (1985) 375–376.
[26] P. Carter, L. Abrahmsen, J.A. Wells, Probing the mechanism and improving the rate of substrate-assisted catalysis in subtilisin BPN, Biochemistry 30 (1991) 6142–6148.
[27] L. Abrahmsen, J.A. Wells, Engineering subtilisin its substrates for efficient ligation of peptide bonds in aqueous solution, Biochemistry 30 (1991) 4151–4159.